

Translation-enriched Z_2 spin liquids and topological vison bands: Possible application to α - RuCl_3

Xue-Yang Song¹ and T. Senthil¹

¹*Department of Physics, Massachusetts Institute of Technology, MA 02139, USA*

(Dated: July 25, 2022)

Inspired by experiments on the magnetic field induced phases of the spin-orbit coupled $2d$ Mott insulator α - RuCl_3 , we study some general aspects of gapped Z_2 Quantum Spin Liquids (QSL) enriched by lattice translation symmetry. We show that there are 12 distinct such phases with different implementations of translation symmetry. In some of these phases the vison excitations of this QSL may form topological Chern bands. We explore a phenomenological description of a putative Z_2 QSL as a candidate ground state at intermediate magnetic fields in α - RuCl_3 . This state has broad continuum spectra in neutron scattering, a “bosonic” thermal Hall signal that goes to zero at zero temperature, and is naturally proximate to a zigzag magnetic ordered state, all of which are also seen in α - RuCl_3 . On general grounds continuum scattering will also be seen at multiple points in the Brillouin zone in this state.

The search for a Quantum Spin Liquid (QSL) state in electronic materials has led to intensive study of α - RuCl_3 in the last few years[1–5]. This is a layered material with spin-orbit coupled $J = 1/2$ moments arranged on a honeycomb lattice in each layer. α - RuCl_3 is deemed a ‘Kitaev material’[6] where the dominant interactions yield a Hamiltonian whose exact solution[7] (by Kitaev) reveals a quantum spin liquid phase. Like many other Kitaev materials, the moments of α - RuCl_3 order magnetically (into a zigzag pattern) at low temperature due to the effect of other interactions beyond the exactly solvable model. The magnetic ordering is suppressed by application of a modest in-plane field of about $B_c \approx 7T$. Attention has thus shifted to the possibility of a QSL phase at intermediate fields just beyond B_c before the onset of the expected phase smoothly connected to the fully spin-polarized paramagnet.

In the region between $B_c \approx 7T$ and about $9T$, a number of phenomena have been found which hint at a possible QSL state. Most intriguing is the observation of a large thermal Hall signal even when the magnetic field is strictly in-plane. Early measurements suggested a quantized thermal Hall conductance[8, 9] consistent with that expected for a specific field-induced non-abelian QSL state (known as the Ising anyon state) in the ideal Kitaev model. Subsequent experiments[10] however report an unquantized, strongly temperature dependent, thermal Hall effect that at higher fields could be understood as coming from a topological magnon found in spin wave calculations of the fully polarized state[11–14]. The Hall signal is seen when the field is applied along the $[11\bar{2}]$ direction in the coordinate system of the underlying octahedra[15] (i.e. the a axis in fig2(a), perpendicular to a honeycomb bond), and is absent when the field is along $[\bar{1}\bar{1}0]$, parallel to the bonds (the b axis). This is consistent with the presence of a π rotation symmetry C_{2b} in the latter case. For a $[11\bar{2}]$ field, the only symmetry that is preserved is lattice translation (and $C_{2b}\mathcal{T}$ where \mathcal{T} is time reversal) and a non-zero thermal Hall effect is not forbidden.

The observed[10] suppression of the thermal Hall effect

with decreasing temperature calls into question the scenario of the field induced non-abelian Ising anyon state of the ideal Kitaev model. Nevertheless spectroscopy measurements do not observe any sharp peaks but just a broad continuum scattering at fields just beyond B_c [16–19] keeping hopes alive for some kind of field-induced QSL, even if not the Ising anyon state. Both neutron[17, 18] and thermodynamic measurements[20, 21] are consistent with an excitation gap, and thus the possibility of a gapped spin liquid at intermediate B . Microscopically a realistic model[6, 22, 23] of α - RuCl_3 must supplement the Kitaev term with other terms, including Heisenberg and anisotropic interactions which are not too small. The phase diagram of such a model in an in-plane field is not known reliably, despite important numerical studies on small system sizes[15]. Available results show that the exactly soluble spin liquid state is destabilized by these other terms; instead magnetically ordered states and indications of other QSL states are found. Thus the existence of a QSL ground state in α - RuCl_3 remains a tantalizing, but hardly settled, possibility.

Motivated by this state of affairs, we consider a simple gapped Z_2 QSL, enriched by lattice translation but no other global symmetries, as a candidate ground state for α - RuCl_3 in a generic field direction (including $[11\bar{2}]$)¹. We explore the idea that the thermal hall signal may originate from topological bands of fractional excitations called visons of such a QSL. Ref [24] considered thermal Hall effects from visons (really non-abelions) of the Ising anyon state from perturbing the Kitaev model, where visons form Chern bands leading to a large thermal Hall signal at intermediate temperatures. Eventually though, at the lowest T , the quantized Majorana fermion thermal Hall conductivity will result. Here we instead study ordinary Z_2 QSLs with no quantized thermal Hall conductivity in the low- T limit.

¹ $C_{2b}\mathcal{T}$ is broken by B along generic directions but preserved by $B \parallel [11\bar{2}]$. We ignore $C_{2b}\mathcal{T}$ in most of our discussion and account for it in a phenomenological model presented later.

We first classify all such translation enriched gapped Z_2 QSLs in $2d$. We find 12 distinct translation symmetric Z_2 QSLs. In some of these translation acts by permuting topologically distinct quasiparticles. We identify general principles that allow visons to form a band with nonzero Chern number. These formal considerations will be helpful in interpreting experiments and numerics on Kitaev materials and their models. As an application, we explore a phenomenological description of α -RuCl₃ in an intermediate strength [11 $\bar{2}$] field as a particular Z_2 QSL where translation along one direction permutes topological quasiparticles. This state is naturally proximate to the zigzag orders at low fields. It accommodates vison Chern bands resulting in a thermal hall signal consistent with observations. We comment on the relationship with the thermal hall effect at larger B which is likely due to topological magnons. This QSL will have continuum scattering in neutron spectroscopy with a characteristic periodicity within the Brillouin zone as an experimental signature. The possibility of a non-Kitaev Z_2 QSL has been explored before[25] with the full space group symmetries of honeycomb lattices and time reversal as a candidate for a ‘proximate’ zero-field spin liquid in RuCl₃.

Translation-enriched Z_2 QSL classification Z_2 QSLs are topologically ordered and have two distinct bosonic gapped anyon excitations e, m with π mutual statistics in a $2D$ system. The fusion rules are

$$e \times e = 1, m \times m = 1, e \times m = \epsilon \quad (1)$$

with the ϵ a fermion (with π mutual statistics with either e or m). Consider the realizations of such QSLs on a lattice with symmetry under elementary translations along 2 primitive lattice vectors $T_{1,2}$, the angle between which are taken to be smaller than or equal to 90° . Despite the tremendous progress in classifying symmetry enriched topological ordered (SET) states[26–30] from diverse approaches, for translation symmetries, only partial results are available in the published literature. Here we use a physical approach to find all distinct translation enriched Z_2 QSLs in a $2D$ system.

In classifying SET states, it is convenient to ask about the action of the symmetry on the topological quasiparticle excitations. There are two distinct situations which require separate treatments. First, the symmetry action does not permute any anyons. Then we can discuss the action of the symmetry on each anyon species separately. This action may be projective, i.e., the symmetry may be fractionalized by the anyon. Distinct SET states are obtained by assigning distinct projective representations to the various anyons together with some consistency requirements. The second case - the symmetry action includes a permutation of anyons. The anyons being permuted must have identical topological properties for this to be allowed. For the Z_2 QSL, this means that some translation could act by interchanging the e and m particles. A number of examples have been constructed of such anyon exchange by translation. Examples in-

clude the strong bond limit of the Kitaev model[7], the Wen plaquette model[31], as well as recent constructions obtained by decorating lines on the lattice with $1d$ topological superconductors formed by the ϵ particles[30, 32].

In general all physical (local) operators should obey $T_1 T_2 T_1^{-1} T_2^{-1} = 1$. Restricting first to the simpler situation in which anyons are not permuted under translation (dubbed as type A), the e (or m) could transform with $T_1 T_2 T_1^{-1} T_2^{-1} = \pm 1$. A -1 factor is the only allowed possibility, such that the physical states with 2 identical anyons (eq (1)), still follow a linear representation of translations. Whether the translations act linearly or projectively can be chosen independently for the e and m particles, apparently giving four distinct choices. However keeping in mind that the label e and m can be interchanged without changing the phase, there is a unique phase where translations act projectively on one of e, m and linearly on the other. Thus we have 3 distinct Z_2 QSLs where translations do not permute anyons. To explicitly construct anyon models that realize all of these possibilities we consider Z_2 gauge theories with background e or m charges placed on all the unit cells of the lattice[33, 34] (see Table I and Fig 1). Note that the phase labeled A^ϵ can be understood as having a background ϵ anyon at each site of the lattice.

Next we turn to translations that permute e and m particles. Now either only one of the two translations T_1 (type B) and T_2 (type C) may permute these anyons or both of them may do so (type D). In all cases we can find a larger translation T_i that preserves the anyon type. We then focus on ‘elementary’ T_i ’s which generate all translations that act on a particular anyon without permuting it to a different anyon. For example, for Wen’s plaquette model[31] plotted in fig 1 (2) where translations permute e, m , the T_i ’s are taken to be $T_1 T_2^{\pm 1}$ indicated by the dashed lines. T_i ’s are the elementary translations for plaquettes where e or m anyons live, i.e. a checkerboard pattern on the square lattice. When translations permute e, m , phases are distinguished by whether T_i ’s are realized linearly or projectively, as listed in Table I. When different anyon sectors are connected by translations, e, m must transform in the same manner - translations either commute or anti-commute, denoted by a superscript \pm attached to the translation types B, C, D .

Finally let us consider phases obtained by placing a background ϵ anyon at each site. We argue that for B^+, C^+, D^+ types, this generates new phases while for B^-, C^-, D^- it does not. Translation T_i permuting e, m can be realized by placing a series of Kitaev chains[35] along the transverse direction, which induces a Majorana when a π flux (e, m) tunnels across the wire, and exchanges e, m [30, 32]. Now for the $+$ phases, consider the allowed ground states on a torus with $L_x L_y$ unit cells ($L_{x,y}$ the number of sites along x and y directions respectively), and add a background ϵ on each site: to conserve fermion parity per the gauge constraint, the boundary conditions (BC) for the Kitaev wires should be changed so that there is an extra π flux compared to when there

Type	$T_{1\bar{2}}^e$	Defining relations on e, m	Model
A^+	1		$T_{1\bar{2}}^{e(m)} = 1$ 1: $n_{e(m)} = 1(0)$
A^-	-1		$T_{1\bar{2}}^{e(m)} = \pm 1$
A^ϵ	1	not for odd $L_x L_y$	$T_{1\bar{2}}^{e(m)} = -1$ 1: $n_\epsilon = 1$
B^+	1	$T_{\bar{1}} = T_1^2$	3
B^-	-1		$T_{1\bar{2}}^{e(m)} = -1$ 3: $n_{e(m)} = 1$
B^ϵ	1	BC change	$T_{1\bar{2}}^{e(m)} = 1$ 3: $n_\epsilon = 1$
C^+	1	$T_{\bar{2}} = T_2^2$	3
C^-	-1		$T_{1\bar{2}}^{e(m)} = -1$ 3: $n_{e(m)} = 1$
C^ϵ	1	BC change	$T_{1\bar{2}}^{e(m)} = 1$ 3: $n_\epsilon = 1$
D^+	1	$T_{1,\bar{2}} = T_1^{\pm 1} T_2$	$T_{1\bar{2}}^{e(m)} = 1$ 2
D^-	-1		$T_{1\bar{2}}^{e(m)} = -1$ 2: $n_{e(m)} = 1$
D^ϵ	1	BC change	$T_{1\bar{2}}^{e(m)} = 1$ 2: $n_\epsilon = 1$

TABLE I: Classification of Z_2 QSLs with translations. Naming rules: (A) translations preserve anyon types, (B) only T_1 , and (C) only T_2 permutes e, m and (D) $T_{1,2}$ both permute e, m . Superscript \pm, ϵ denotes no background anyon, background m, e or a background ϵ per site, respectively. Defining relations $T_{ij}^{\epsilon, e, m} = T_i T_j T_i^{-1} T_j^{-1}$ for anyons are listed. Models 1, 2, 3 are shown in fig. 1. Translation types B are realized by rotating model 3 by 120° clockwise. $n_{e, m, \epsilon}$ are the number of e, m, ϵ per site/plaquette which has default value 0 unless specified in the table.

was no background added ϵ charge. This change in the allowed ground states on such a torus is probed by asking about the phase seen by the ϵ as it is dragged around the appropriate cycle of the torus. Hence we conclude that these are new SET classes. Stacking ϵ per site, however, does not change the defining relations for e, m of modified $T_{\bar{i}}$, as the trajectory for the relations enclose an even number of ϵ 's. For SET B^-, C^-, D^- where background e, m exists, the additional ϵ can be combined with background visons and does not give new SET classes². We name these classes with background ϵ on each site with a superscript ϵ in table I.

We thus have 12 translation-enriched gapped Z_2 QSLs in 2d, listed in table I. To construct models for each SET class we use the 3 prototypes in fig 1 to realize different translation types with details in Appendix A.

In passing, we note that we can readily generalize the classification to $3+1D$ Z_2 topological order with point-like bosonic e particles and tensionful unoriented vison loops as fractional excitations. We show in Appendix E[36, 37] that there are 128 symmetry enriched Z_2 QSLs in $3D$, distinguished by defining relations on e , vison loops and decorating lattice planes with $2d$ symmetry protected topological states of the bosonic e -particles.

² Here the criterion of BC change does not apply since a consistent assignment of background e, m to each plaquette, requires even dimension along the direction that permutes e, m .

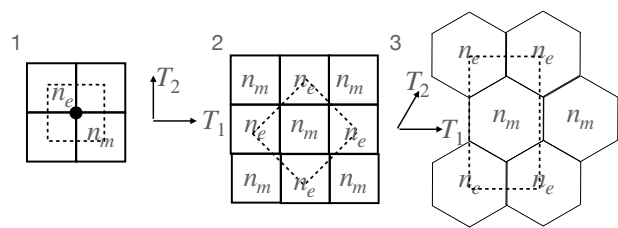


FIG. 1: The model for Z_2 QSLs that realize the 12 SET classes in table I. Model 1, 2, 3 are toric code[38], Wen's plaquette model[31] and the strong bond limit of the Kitaev model, respectively. $n_{e, m} = 0, 1$ are the number of visons in each model. ϵ lives on site (or slightly displaced if coincides with e). Dashed lines display the trajectory an anyon takes in the defining relation in table I.

Armed with this understanding we turn next to the question of which of these $2d$ Z_2 QSLs admits vison Chern bands. A quadratic Hamiltonian provides an adequate description of the gapped visons, so that the notion of a Chern number is well defined for the resulting bands. We prove in Appendix C[39–41] that since translation-invariant SETs where translations commute on anyons, are governed by an explicitly translation-invariant Hamiltonian, no vison Chern band is possible if the visons hop on a primitive Bravais lattice.

The presence of background anyons, if any, leads to a braiding phase seen by other anyon species on any path that encloses an odd number of the background anyons, with discussions for generic Z_2 QSLs in Ref [42]. Specifically if we consider, eg, hopping of an e particle,

$$\text{Sign}[\prod_{ij \in p} t_{ij}] = (-1)^{n_p} (-1)^{l_p}, \quad (2)$$

where p is any path formed by vison hopping t_{ij} , l_p the number of hops along p , and n_p the number of background anyons (m or ϵ) enclosed by p .

Topological bands from fully frustrated visons- A common spin liquid state constructed by parton constructions for spin-1/2 operators (Schwinger boson or Abrikosov fermion) has one 'spinon' per site, conveniently viewed as a background anyon of some fixed type. Without loss of generality we take this background anyon to be either an e or ϵ particle. In such an SET state the visons (m particles) are described by a fully frustrated Ising model(FFIM) on the dual lattice[33, 34, 43, 44]. The frustration is a direct consequence of the braiding phase of m around the background anyon.

We construct (projective) translation invariant models for visons on 3 kinds of lattices which exhibit Chern bands. The Hamiltonian for the visons formally reads,

$$H_v = \sum t_{ij} v_i^\dagger v_j + \sum \Delta_{ij} v_i^\dagger v_j^\dagger + h.c., \quad (3)$$

where v_i^\dagger is a vison creation operator at site i . Pairing is added since vison numbers are conserved modulo 2.

On dual square, honeycomb lattices, the hopping flux around an elementary plaquette is π for visons to be frustrated, while on triangular lattices the flux is 0 and on kagome lattices flux is $0, \pi$ for triangle/hexagon plaquettes, respectively. Hence the translations for visons anticommute on square, honeycomb and kagome lattices. Translations, however, commute on triangular lattices. This shows that it is impossible to have a Chern band on triangular FFIM. We list the model with topological vison bands and the typical Berry curvature distribution in appendix D. This exercise demonstrates (not surprisingly) that band topology of visons is possible as a matter of principle in Z_2 QSLs. Whether it is actually realized is a question to be answered by calculations on microscopic models or through experiment.

Application to α -RuCl₃: Microscopic calculations on realistic models (significantly different from the pristine Kitaev model) of α -RuCl₃ are difficult and beyond the scope of this work. We will instead develop a phenomenological model for the vison bands that, as will see, accommodates some of the key experimental features of this material³. Specifically we introduce a vison model on the honeycomb lattice where one translation T_2 permutes e, m . To have nontrivial vison band topology, we consider background anyon flux as a source of projective translation for the visons and assign e, m to live in hexagons in alternate rows along T_2 . This falls into SET class C^- . Besides hopping and pairing, a staggered chemical potential is added to reflect the weak translation breaking for visons and dynamically suppress nearest neighbor hopping of e or m along T_2 which excites an ϵ . Fig 2 shows the model with translations and $C_{2b}\mathcal{T}$, band structure and κ_{xy}/T (details in Appendix B[51]).

There are 3 advantages to this construction: 1) A key feature of the putative intermediate field QSL is its proximity to the zigzag magnetically ordered phase at low B , which breaks one translation T_2 and preserves T_1 (also $C_{2b}\mathcal{T}$ if ordered in $a-c$ plane). This is the only distinction from the QSL phase symmetry-wise. Since condensing e or m would break T_2 , this model naturally accounts for the zigzag phase at small B that preserves $T_1, T_2^2, C_{2b}\mathcal{T}$ provided visons condense at the Γ point, which may be natural for small B . 2) The topological vison band structure allows a thermal Hall effect that will decrease to zero as $T \rightarrow 0$. The change of sign in κ_{xy} when B flips direction in the ab plane is guaranteed since this corresponds to the time-reversal breaking terms for visons to change sign, which changes the sign of the Berry curvature and hence κ_{xy} . This route to the thermal Hall signal is similar to that in the topological magnon theory, which presumably applies at higher

fields beyond the proposed QSL regime). Heuristically as B is decreased the magnons fractionalize into visons upon entering the QSL; it is perhaps not surprising that the resulting vison bands inherit a band topology from the parent magnons. On the technical side, despite the resemblance to the theory of topological magnon bands, the presence of background anyon flux allows frustrated hopping for e, m , and hence offers more possibility for development of Chern bands for visons. 3) The fractionalization of magnons into visons implies that the neutron scattering signal will be dominated by continuum scattering and will not see sharp peaks. This is indeed what is seen in neutron experiments⁴

A striking experimental signature of the translation-enrichment in this QSL is an enhanced periodicity of the spin structure factor associated with the continuum scattering within the microscopic Brillouin zone. This was discussed in Ref. [53] and readily generalized to situations where translation permutes the anyons. For the specific Z_2 QSL above, the enhanced momenta are discussed in appendix F. Existing experiments show weak signals at these momenta. Our discussion urges further experiments to look for the enhanced periodicity.

Considerations from microscopics A Z_2 QSL where one translation permutes anyons occurs already in a spatially anisotropic deformation of the Kitaev model. This model has no background anyon (i.e zero flux) in the ground state. Realistic models for α -RuCl₃ include a significant additional antiferromagnetic Γ interaction[23] between nearest neighbors, $\sum_{\langle ij \rangle_\gamma} \Gamma S_i^\alpha S_j^\beta$, where α, β are the two remaining spin indices for a γ type bond in Kitaev model. The inclusion of the Γ terms stabilizes an apparently distinct QSL dubbed *KTSL* in Ref [15], with a negative flux expectation value ($\langle W_p \rangle$). If this is a Z_2 QSL, this signals a state with background vison numbers $n_{e,m}$ per plaquette. The phase diagram in a field is highly sensitive to small perturbations (anisotropic interactions and Heisenberg exchange). It is conceivable that for some choice of parameters a Z_2 QSL may emerge at intermediate fields, distinct from that associated with the exactly solvable Kitaev model (as the existence of *KTSL* already demonstrates). Our general discussion of translation enriched topological order helps identify such a QSL in future studies of microscopic models.

Conclusion Motivated by indications for an intermediate-field QSL in α -RuCl₃, we studied some general properties of gapped Z_2 QSLs with no global symmetries other than lattice translations. Building on prior partial results we classified such QSLs, and identified situations in which visons (e and m particles) form topological Chern bands. We discussed some phenomenologically attractive features of such gapped Z_2 QSLs with vison Chern bands: continuum scattering

³ Some thermal Hall measurements in an out-of-plane B [45] are proposed to be due to phonons. Theoretically the relevance of phonons to thermal hall in diverse systems have been investigated [46–50]; here, the phonon origin is inconsistent with the κ_{xy} scale and temperature dependence in α -RuCl₃[10]

⁴ In contrast ESR [52] sees sharp resonances even in the putative QSL region, at frequencies accessible to neutron spectroscopy. It is unclear at present how to reconcile these two observations.

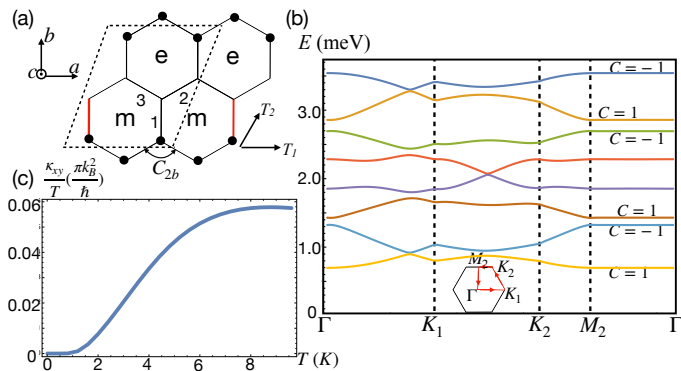


FIG. 2: (a) The honeycomb vison model for e with an 8-site unit cell and Chern bands, where translation T_2 permutes e, m . Visions live on-site and hop in a background anyon flux marked in hexagons. e, m see $\pi(0), 0(\pi)$ flux per hexagon in alternate rows along T_2 , respectively. Hence the hopping and pairing are negative for e on the red bonds. The nearest-neighbor hopping strength is 0.4meV , pairing amplitude 0.28meV and phase $0, \pm 2\pi/3$ for bond types 1, 2, 3, respectively. Chemical potential $-2 \pm 0.4\text{meV}$ for sites with (without) black dot markers, respectively. The model for m is obtained by applying T_2 on model for e . (b) The dispersion of all 8 gapped vison bands along high symmetry lines in the reduced Brillouin zone. Band touching appears between 4th and 5th bands. Chern numbers for other bands are marked. (c) The thermal Hall conductivity of e, m in the vison model. The value of κ_{xy}/T is comparable to results in ref [10].

in neutron spectroscopy, a thermal Hall effect that decreases to zero with temperature, and a natural connection to zigzag magnetic ordering. The models discussed naturally have images of the continuum scattering at multiple locations in the Brillouin zone. Our discussion is phenomenological, and making contact with microscopic calculations will be important moving forward. On the theoretical front, the critical confinement (Higgs) transition from the specific Z_2 QSL discussed to the zigzag phase would be interesting to study numerically. Closely related transitions have been studied numerically [54] with fascinating results that are yet to find a field theoretic understanding.

Acknowledgements: We thank Stephen Nagler, Hae-Young Kee and Subir Sachdev for useful discussions. We also thank Hae-Young Kee for a careful reading and comments on an earlier version of the paper. X-Y Song thanks discussion with Yi-Zhuang You, Tarun Grover and John McGreevy. X-Y S is supported by the Gordon and Betty Moore Foundation EPiQS Initiative through Grant No. GBMF8684 at MIT. This work was supported by NSF grant DMR-1911666, and partially through a Simons Investigator Award from the Simons Foundation to Senthil Todadri. This work was also partly supported by the Simons Collaboration on Ultra-Quantum Matter,

which is a grant from the Simons Foundation (651440, TS).

Appendix A: Symmetry enrichment of Z_2 topological order with translations

Here we list the model construction plotted in fig 1 of the main text for the realizations of different translation-enriched SETs.

To realize the defining relation i.e. projective symmetry group (PSG) in each SET class, we utilize the fact that e, m have mutual π braiding statistics. An adiabatic evolution around the other type of anyon could be realized by the translation operation $T_1 T_2 T_1^{-1} T_2^{-1}$. Hence the phase factor ± 1 in the relation depends if the trajectory of the translation operation encircles an odd number of anyons of the other species. The anyon occupation can be tuned by adjusting the chemical potential for the anyons.

For type $A^{\pm, \epsilon}$, we look to the original Kitaev toric code model where Z_2 gauge field σ^z lives on the square lattice bonds [7].

$$H_{tc} = \mu_m \sum_{i \in P} \prod \sigma_i^z + \mu_e \sum_{i \in v} \prod \sigma_i^x, \quad (\text{A1})$$

where P, v denote the elementary plaquette and the vertices, respectively. $\mu_{m, e}$ are the chemical potential for an m, e excitation, respectively. When $\mu_{m, e} > 0$, the ground state is the vacuum and the translations on the visons permute. When $\mu_m \mu_e < 0$, the ground state contains one e or m particle per unit cell depending on which chemical potential is negative. Hence the translations for m or e anti-commute due to the mutual semion statistics of the visons. Note this gives one unique SET class A^- since one can always define the vison that has anti-commuting translations to be e.g e particles.

When $\mu_m < 0, \mu_e < 0$, there is one e and m (identically an ϵ) per unit cell, and translations for both anyons anti-commute, hence type A^ϵ .

For the model where one translation permutes e, m , we look to a variant of the toric code model as discussed in sec 7.1 of ref [7]. Plotted in fig 1(3) of the main text, the e, m particles live in alternate rows of the honeycomb lattice. One again tunes the chemical potential. When $\mu_{e, m} > 0$, the ground state has no anyon charge and translations for anyons commute. When $\mu_m = \mu_e < 0$, there is one e and m per unit cell, and translations for both anyons anti-commute, hence class C^- . Note the chemical potential for e, m should be equal due to the translation that permutes the anyons. One may ask if the projective relation could be different for e, m . It is indeed possible when neither translation permutes anyons that e, m obey different projective translations. Hence type (a) further classifies into 3 cases where both/neither anyon transform projectively (i.e. two translations commute), or one of 2 anyons transform projectively. Type B^\pm can be similarly obtained

by rotating the model in fig 1(3)(main text) 120° . Such a Z_2 topological order can be constructed on the square lattice, e.g. by coupling together 1d Kitaev chains and gauging the fermion parity[30, 32].

When both translations permute e, m , we take Wen's plaquette model[31]. The Z_2 variables live on the sites and the Hamiltonian reads,

$$H = \mu \sum \prod_{i \in A} \sigma_i^z + \sum \prod_{i \in B} \sigma_i^x, \quad (\text{A2})$$

where A, B denote the elementary plaquettes that organize into a checkerboard pattern on square lattice as plotted in fig 1 (2) in the main text. $\mu > 0$ yields a trivial ground state and class D^+ . $\mu < 0$ gives one vison per plaquette as the ground state and translations anti-commute, hence class D^- .

For classes with superscript ϵ , they can be readily realized by the corresponding model (toric code for A , model 3 for B, C and Wen's plaquette model for D , respectively) by placing one ϵ per site.

Appendix B: Thermal hall from a vison Chern band

The thermal hall conductivities from bosonic particles arise from integral of the Berry curvature[39] multiplied by energy-dependent functions[51]. Hence generally a band of nontrivial Chern number will give notable thermal hall conductivity.

$$\kappa_{xy} = \frac{2k_B^2 T}{\hbar V} \sum_{n, \mathbf{k}} c_2(\rho_n) \text{Im} \left\langle \frac{\partial u_n}{\partial k_x} \middle| \frac{\partial u_n}{\partial k_y} \right\rangle. \quad (\text{B1})$$

, where $\rho_n \equiv \rho(\epsilon_{nk})$ and $c_2(\rho) = (1 + \rho)(\log \frac{1+\rho}{\rho})^2 - (\log \rho)^2 - 2\text{Li}_2(-\rho)$, $\text{Li}_2(z)$ is the polylogarithm function.

When calculating the thermal hall conductivity for the model we propose in the context of α - RuCl_3 , the different bands are not completely isolated from each other. The band touching points are described by (single particle) Dirac Hamiltonians and the thermal hall contribution of the corresponding states vanishes. These states have the same energy and the Berry curvature adds to 0 in proximity of the Dirac point.

Appendix C: Translation-commuting vison models have trivial band topology

We prove that in the SET classes where translations commute, i.e. class $A^{+, \epsilon}, B^{+, \epsilon}, C^{+, \epsilon}, D^{+, \epsilon}$ in Table I of the main text, it is impossible to generate Chern bands when the visons hop on a unit cell with just one site. For SETs where translations permute anyons, we consider effectively only the part of the lattice where a particular anyon lives and a model on the effective lattice, since e, m cannot mix as they live in different superselection

sectors. Then the composite translation T_i^z that we use in Table I of the main text for classes IV, VI, VIII act as elementary translations on the effective lattice.

First in a projective relation of translations $T_{1,2}$ where the gauge group is Z_2 , the phase for $T_1 T_2 T_1^{-1} T_2^{-1}$ is equivalent to the hopping flux along the trajectory p of a certain site acted on by $T_1 T_2 T_1^{-1} T_2^{-1}$, i.e.

$$\text{Arg}[T_1 T_2 T_1^{-1} T_2^{-1}] = \text{Arg}[\prod_{l \in p} t_l]. \quad (\text{C1})$$

Note that the hopping t_l is oriented along the trajectory of the site. Consider a projective translation by a vector \mathbf{v} ,

$$T_v : c_i \rightarrow e^{i g_v(i)} c_{i+\mathbf{v}}, \quad (\text{C2})$$

where a phase is encoded in the function g_v . Then for a site i

$$\text{Arg}[T_1 T_2 T_1^{-1} T_2^{-1}] = (g_1(i) - g_1(i + \mathbf{l}_2)) + (g_2(i + \mathbf{l}_2) - g_2(i)). \quad (\text{C3})$$

One further knows that for the translation to keep the hopping invariant i.e.

$$T_v : c_i^\dagger c_j \rightarrow e^{i(g_v(i) - g_v(j))} c_{i+\mathbf{v}}^\dagger c_{j+\mathbf{v}}, \quad (\text{C4})$$

the phase difference satisfies

$$g_v(i) - g_v(j) = \text{Arg} \left[\frac{\prod_{l \in i+\mathbf{v} \rightarrow j+\mathbf{v}} t_l}{\prod_{l \in i \rightarrow j} t_l} \right], \quad (\text{C5})$$

where the hopping amplitude is multiplied along a (series of) bonds l that connect i, j .

Combining eqs (C3) and (C5), we prove eq (C1).

For the SET classes where translations commute, it is always possible to choose a gauge such that all t_l around the trajectory p is real and positive, so that the flux to be 0. In this case, the translation action is trivial, i.e. $g_v = 0$ identically. It is still true even with vison pairing or hopping beyond nearest-neighbor.

Hence the vison model is explicitly translation invariant. In this case, if the unit cell on which the vison moves contains only one site, the reciprocal space Hamiltonian is factorized as

$$H(\mathbf{k}) \equiv e^{-i\mathbf{k} \cdot \mathbf{R}} H(\mathbf{r}) e^{i\mathbf{k} \cdot \mathbf{R}} = h(\mathbf{k}), \quad (\text{C6})$$

where \mathbf{R} is the Bravais lattice location that labels unit cells. This is a single band system and the Berry curvature /Chern number vanishes. This still holds if one adds pairing. Suppose the Hamiltonian reads in momentum space (with the spinors $\psi_k = (c_k, c_{-k}^\dagger)^T$),

$$H(\mathbf{k}) = \psi_k^\dagger h_k \psi_k \quad (\text{C7})$$

where $\sigma^1 h_k^* \sigma^1 = h_{-k}$ is a 2×2 Hamiltonian. The two bands are split into a particle and hole band, respectively [11, 40, 41] where each band contains the full information

of the system due to the redundancy relating h_k, h_{-k}^* . The Chern number sum for the particle/hole band is 0[40], which in our case means the single band holds a trivial Chern number. Hence we have proved that no Chern band is possible for translation commuting SETs. This does not exclude a nonzero thermal hall conductivities since κ_{xy} is a weighted sum of the Berry curvature, though it could guide the search for topological vison bands which more naturally contribute to thermal hall effects.

Appendix D: Models with topological vison bands in fully frustrated Ising paramagnets on honeycomb, kagome and square lattices

For simplicity, for FFIM we mainly consider vison hopping (including small pairing will not change band topology).

The symmetries of interests are translations only, which constrains that the hopping flux for visons should be translation invariant. We specialize to the case where the visons live on the plaquettes of the original lattice which is natural in the parton construction. Furthermore the parton construction for spin-1/2 systems gives natural access to phases where the vison hopping are frustrated as described in eq (3) of the main text. We construct a hopping model to demonstrate the possibility of Chern bands.

The hopping amplitudes t_{ij} are plotted in fig 3 by arrows (imaginary hopping) and colors of the bonds (real hoppings). The model is complemented by imaginary hoppings that breaks time reversal, necessary for nontrivial band topology. We plot the Berry curvature distribution for one of the Chern bands on Honeycomb and Kagome lattices in fig 4. On square lattices, the model is the familiar spinon mean-field ansatz for a chiral spin liquid that holds a Chern band.

Appendix E: Translation SET classification for (3+1)D Z_2 topological orders

In 3+1D Z_2 topological orders there are gauge charges e and vison loops m . Clearly translations cannot permute particles and loops. We limit the discussion to cases where the gauge charge e is a boson.

Take a cubic lattice with translations along 3 orthogonal directions $T_{1,2,3}$ for example where e lives on the sites. There are 3 projective translation relations for e , $T_i T_j T_i^{-1} T_j^{-1} = \pm 1$ where $T_{i,j} (i, j \in [1, 2, 3])$ are any 2 orthogonal translations of the 3 elementary translations. The phase factor depends on the Z_2 gauge flux per plaquette in the plane defined by $T_{i,j}$. In total there are $2^3 = 8$ classes from translations on e . Similarly new SET classes are obtained by asking if a gauge charge is placed at each site. Having 1 gauge charge per site in the background will manifest in the translation of vor-

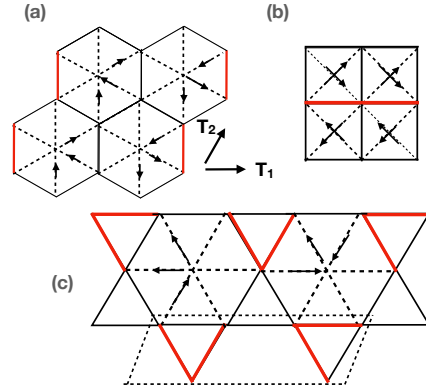


FIG. 3: The fully frustrated vison hopping model that yields a Chern band on honeycomb, square and kagome lattices. The model is translation invariant as the hopping flux around any kind of plaquette is translation invariant. The arrows from $i \rightarrow j$ indicate imaginary hopping $ic_i^\dagger c_j$ and solid black/red lines indicate real positive/negative hopping, respectively. (a) On honeycomb lattice we take the next-nearest-neighbor (NNN) imaginary hopping to be large that effectively realize a chiral spin liquid on triangular lattices. The nearest-neighbor (NN) hopping satisfy the fully frustration condition. (b) On square lattice the FFIM hop in π flux and the diagonal imaginary hopping yields a Chern band. (c) For Kagome lattices the NN hopping is real and diagonal hopping imaginary indicated by the arrows.

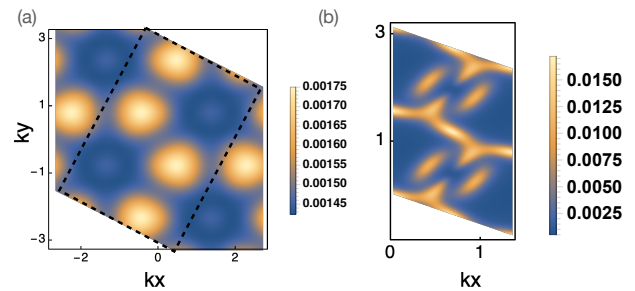


FIG. 4: Berry curvature for the honeycomb (a) and kagome (b) vison model (FFIM) plotted in fig [?] which give a Chern number of 1, 3, respectively. Dashed square in (a) and the region plotted in (b) is the reduced Brillouin zone as the unit cell is enlarged by a factor of 2 for the FFIM. There is a C_6 rotation for the FFIM on honeycomb lattice we consider.

tex loops: Consider a vortex loop along e.g. the T_1 direction in a system with odd dimension L_1 along T_1 , and move it by $T_2 T_3 T_2^{-1} T_3^{-1}$: it will then accumulate an $L_1 \pi \bmod 2\pi = \pi$ Berry phase from encircling the gauge charges on L_1 sites. Hence we can view the Berry phase $0, \pi$ of vortex loop translation under this particular setting as corresponding to decorating each lattice site with either none or a single e particle, i.e. to placing 0 + 1-dimensional Symmetry Protected Topological (SPT) states of the e particles on lattice sites. In total there are 16 classes for 3D Z_2 translation SET orders from placing background gauge charges or flux loops.

Following ideas similar to our discussion in 2 + 1-d, further distinct phases can be obtained by decorating lines with 1 + 1-d SPTs, or planes with 2 + 1-d SPTs of the e particles. However there are no 1 + 1-d SPT states protected by Z_2 symmetry. In 2 + 1-d there is a well-known boson SPT state with Z_2 symmetry which is nicely illustrated by the Levin-Gu model[36].

Gauging the Levin-Gu model leads to the so-called double-semion state, where a π flux is a semion with $\pi/2$ self statistics and when binding with a gauge charge becomes an anti-semion. Stacking these SPTs of the e -particles, in e.g. 1 – 2 plane along the T_3 direction, will result in a semion excitation at the core of a vison loop every time it crosses a 1 – 2 plane. This can be probed by considering two vison loops linked with a dislocation half-plane (1 – 2 plane) with a Burger's vector of a unit vector along T_3 . In the 2-loop braiding process linked with a dislocation plane[37], where one loop first shrinks and goes through the other loop, and then enlarges and crosses back (encompasses) the other loop again, the 2 semions trapped at the half-plane go through a 2π braiding process resulting in a π berry phase coming from their statistics. Next consider combining such a stack of e-SPTs on planes with background π flux through each plaquette. Then a semion will be bound on each plaquette. Again a vison loop linked with a dislocation half-plane (where the e-SPT lives) will see a π Berry phase when moving around a plaquette with a background semion. Similarly combining stacking the e-SPT on planes with states with background e-particles on sites will make the 3-loop braiding when linked with a dislocation half-plane dependent on how many sites with gauge charges are encircled and reflect the additional contribution of the semion trapped in the vison loop as well. Hence we conclude that stacking along three directions gives another $2^3 = 8$ possibilities (independently) on top of placing background fractional excitations. The stacking of e-SPT can be probed by linking a vortex loop with a dislocation half-plane and consider its projective translation or braiding with another loop as described above.

Another potential bosonic SPT state is the E_8 state[7] with a thermal hall conductivity $\kappa_{xy}/T = 8\frac{e^2}{h}$. If one imposes a Z_2 symmetry of boson number conservation modulo 2 and gauge it, the π flux of the Z_2 symmetry is a boson. Furthermore we can regard the E_8 state as a

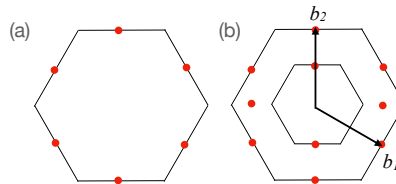


FIG. 5: The momenta at which the enhanced periodicity implies continuum excitations in the spin structure factor (assuming there is such scattering at Γ) for pairs of majoranas (ϵ particles) in (a) and pairs of visons (e, m) in (b) respectively. Due to the anti-commuting relation of $T_{1,2}$ for ϵ and T_2^2, T_1 for e, m , the neutron spectrum is periodic by a momenta transfer of $(0, \pi), (\pi, 0), (\pi, \pi)$ for ϵ and $(\pi, 0), (\pi/2, 0)$ (or sum of the two vectors) for e, m , respectively[53]. (b) also draws the reduced Brillouin zone and reduced reciprocal vectors $b_i \cdot R_j = 2\pi\delta_{ij}$ ($i, j = 1, 2$) for the vison model we use to fit α -RuCl₃. Visons are permuted upon translation T_2 .

combination of the trivial gapped state of the e -bosons together with an E_8 state formed by Z_2 neutral excitations. Hence stacking gauged E_8 states do not really give new SET classes; they merely correspond to the ability to combine the Z_2 SET states with invertible states obtained by stacking layers of the 2 + 1-d E_8 state. We will therefore exclude these from our classification.

In total we have $16 \times 8 = 128$ 3 + 1d SET classes of translation-enriched Z_2 topological order.

Appendix F: Spectroscopic signature of translation symmetry fractionalization in the honeycomb vison model

As discussed in ref[53], the projective representation of translations for visons will result in distinct signature as an enhanced periodicity of the continuum associated with 2-anyon excitations in the spin structure factor. Note that there are three types of continuum spectra that we can expect, associated with exciting pairs of each of the 3 kinds of anyons.

Here we generalize the discussion to cases where translation permute e, m . For the vison model in the main text fig 2, e, m obeys

$$T_1 T_2^2 T_1^{-1} T_2^{-2} = -1, \quad (\text{F1})$$

and ϵ obeys

$$T_1 T_2 T_1^{-1} T_2^{-1} = -1 \quad (\text{F2})$$

due to background anyons. Consider a state with two visons $e_{1,2}$ far away from each other denoted as $|v\rangle$, and

apply T_1 to one of the visons. From the PSG of eq (F1), we have for the momentum along T_2

$$2k_2(|v\rangle) = 2k_2(T_1(e_1)|v\rangle) + \pi, \quad (\text{F3})$$

where $T_1(e_1)$ denotes applying T_1 locally to e_1 only and the factor of 2 appears since T_2^2 is used for the PSG of e . Similarly applying T_2^2 to e_1 , we have

$$k_1(|v\rangle) = k_1(T_2^2(e_1)|v\rangle) + \pi. \quad (\text{F4})$$

Hence we have for the density of states of the two-particle states of e (at a fixed frequency)

$$N_e(\mathbf{k}) = N_e(\mathbf{k} + (0, \pi/2)) = N_e(\mathbf{k} + (\pi, 0)), \quad (\text{F5})$$

in the reciprocal vector basis $b_{1,2}$ marked in fig 5(b) and similarly for m .

For ϵ the case is simpler and follow the analysis in ref [53], we have

$$N_\epsilon(\mathbf{k}) = N_\epsilon(\mathbf{k} + (0, \pi)) = N_\epsilon(\mathbf{k} + (\pi, 0)). \quad (\text{F6})$$

The periodicity of anyon density of states in momentum space will result in the same period in spin structure factor. The spin operator is generally decomposed

to contain vison or ϵ bilinears at leading order in low energy, e.g. for visons one has

$$\mathbf{S}(\mathbf{q}) \sim \mathbf{f}(\mathbf{q}) \sum_k v(k)v(-k + \mathbf{q}) + \mathbf{g}(\mathbf{q}) \sum_k v^\dagger(-k)v(-k + \mathbf{q}) + h.c., \quad (\text{F7})$$

where $\mathbf{f}, \mathbf{g}(\mathbf{q})$ are form factors which generically depend on \mathbf{q} . Hence the spin structure factor probes the two-vison density of states N_e modulated by the form factors. So a period in N_e in momentum space does not lead directly to an exact period in spin structure factor $\langle S(q, \omega)S(-q, -\omega) \rangle$, though one expects the general features in neutron spectroscopy, i.e. peak or continuum, should be repeated qualitatively by a period in vison/ ϵ density of states.

If we assume continuum excitations at the Γ point, as observed experimentally, then the other momenta implied by the enhanced periodicity are marked in fig 5. Note any combination of the periodicity momenta marks also a period.

-
- [1] C Broholm, R.J Cava, SA Kivelson, DG Nocera, MR Norman, and T Senthil, “Quantum spin liquids,” *Science* **367**, eaay0668 (2020).
- [2] Hidenori Takagi, Tomohiro Takayama, George Jackeli, Giniyat Khaliullin, and Stephen E Nagler, “Concept and realization of kitaev quantum spin liquids,” *Nature Reviews Physics* **1**, 264–280 (2019).
- [3] Simon Trebst and Ciarán Hickey, “Kitaev materials,” *Physics Reports* **950**, 1–37 (2022).
- [4] Maria Hermanns, Itamar Kimchi, and Johannes Knolle, “Physics of the kitaev model: fractionalization, dynamical correlations, and material connections,” arXiv preprint arXiv:1705.01740 (2017).
- [5] Stephen M Winter, Alexander A Tsirlin, Maria Daghofer, Jeroen van den Brink, Yogesh Singh, Philipp Gegenwart, and Roser Valentí, “Models and materials for generalized kitaev magnetism,” *Journal of Physics: Condensed Matter* **29**, 493002 (2017).
- [6] George Jackeli and Giniyat Khaliullin, “Mott insulators in the strong spin-orbit coupling limit: from heisenberg to a quantum compass and kitaev models,” *Physical review letters* **102**, 017205 (2009).
- [7] Alexei Kitaev, “Anyons in an exactly solved model and beyond,” *Annals of Physics* **321**, 2–111 (2006), january Special Issue.
- [8] T. Yokoi, S. Ma, Y. Kasahara, S. Kasahara, T. Shibauchi, N. Kurita, H. Tanaka, J. Nasu, Y. Motome, C. Hickey, S. Trebst, and Y. Matsuda, “Half-integer quantized anomalous thermal hall effect in the kitaev material candidate $\alpha\text{-RuCl}_3$,” *Science* **373**, 568–572 (2021), <https://www.science.org/doi/pdf/10.1126/science.aay5551>.
- [9] J. A. N. Bruin, R. R. Claus, Y. Matsumoto, N. Kurita, H. Tanaka, and H. Takagi, “Robustness of the thermal Hall effect close to half-quantization in a field-induced spin liquid state,” arXiv e-prints , arXiv:2104.12184 (2021), arXiv:2104.12184 [cond-mat.str-el].
- [10] Peter Czajka, Tong Gao, Max Hirschberger, Paula Lampen-Kelley, Arnab Banerjee, Nicholas Quirk, David G. Mandrus, Stephen E. Nagler, and N. P. Ong, “The planar thermal Hall conductivity in the Kitaev magnet $\alpha\text{-RuCl}_3$,” arXiv e-prints , arXiv:2201.07873 (2022), arXiv:2201.07873 [cond-mat.str-el].
- [11] Li Ern Chern, Emily Z. Zhang, and Yong Baek Kim, “Sign structure of thermal hall conductivity and topological magnons for in-plane field polarized kitaev magnets,” *Phys. Rev. Lett.* **126**, 147201 (2021).
- [12] P. A. McClarty, X.-Y. Dong, M. Gohlke, J. G. Rau, F. Pollmann, R. Moessner, and K. Penc, “Topological magnons in kitaev magnets at high fields,” *Phys. Rev. B* **98**, 060404 (2018).
- [13] Darshan G. Joshi, “Topological excitations in the ferromagnetic kitaev-heisenberg model,” *Phys. Rev. B* **98**, 060405 (2018).
- [14] Tessa Cookmeyer and Joel E. Moore, “Spin-wave analysis of the low-temperature thermal hall effect in the candidate kitaev spin liquid $\alpha\text{-RuCl}_3$,” *Phys. Rev. B* **98**, 060412 (2018).
- [15] Jacob S. Gordon, Andrei Catuneanu, Erik S. Sørensen, and Hae-Young Kee, “Theory of the field-revealed kitaev spin liquid,” *Nature Communications* **10**, 2470 (2019).
- [16] Arnab Banerjee, Jiaqiang Yan, Johannes Knolle, Craig A. Bridges, Matthew B. Stone, Mark D. Lumsden, David G. Mandrus, David A. Tennant,

- Roderich Moessner, and Stephen E. Nagler, “Neutron scattering in the proximate quantum spin liquid α - rucl_3 ,” *Science* **356**, 1055–1059 (2017), <https://www.science.org/doi/pdf/10.1126/science.aah6015>.
- [17] Arnab Banerjee, Paula Lampen-Kelley, Johannes Knolle, Christian Balz, Adam Anthony Aczel, Barry Winn, Yaohua Liu, Daniel Pajerowski, Jiaqiang Yan, Craig A. Bridges, Andrei T. Savici, Bryan C. Chakoumakos, Mark D. Lumsden, David Alan Tennant, Roderich Moessner, David G. Mandrus, and Stephen E. Nagler, “Excitations in the field-induced quantum spin liquid state of α - rucl_3 ,” *npj Quantum Materials* **3**, 8 (2018).
- [18] Christian Balz, Paula Lampen-Kelley, Arnab Banerjee, Jiaqiang Yan, Zhilun Lu, Xinzhe Hu, Swapnil M. Yadav, Yasu Takano, Yaohua Liu, D. Alan Tennant, Mark D. Lumsden, David Mandrus, and Stephen E. Nagler, “Finite field regime for a quantum spin liquid in α - rucl_3 ,” *Phys. Rev. B* **100**, 060405 (2019).
- [19] Zhe Wang, S. Reschke, D. Hüvonen, S.-H. Do, K.-Y. Choi, M. Gensch, U. Nagel, T. Röm, and A. Loidl, “Magnetic excitations and continuum of a possibly field-induced quantum spin liquid in α - rucl_3 ,” *Phys. Rev. Lett.* **119**, 227202 (2017).
- [20] J. A. Sears, Y. Zhao, Z. Xu, J. W. Lynn, and Young-June Kim, “Phase diagram of α - rucl_3 in an in-plane magnetic field,” *Phys. Rev. B* **95**, 180411 (2017).
- [21] O. Tanaka, Y. Mizukami, R. Harasawa, K. Hashimoto, K. Hwang, N. Kurita, H. Tanaka, S. Fujimoto, Y. Matsuda, E. G. Moon, and T. Shibauchi, “Thermodynamic evidence for a field-angle-dependent majorana gap in a kitaev spin liquid,” *Nature Physics* **18**, 429–435 (2022).
- [22] Jeffrey G Rau, Eric Kin-Ho Lee, and Hae-Young Kee, “Generic spin model for the honeycomb iridates beyond the kitaev limit,” *Physical review letters* **112**, 077204 (2014).
- [23] K. W. Plumb, J. P. Clancy, L. J. Sandilands, V. Vijay Shankar, Y. F. Hu, K. S. Burch, Hae-Young Kee, and Young-June Kim, “ α - rucl_3 : A spin-orbit assisted mott insulator on a honeycomb lattice,” *Phys. Rev. B* **90**, 041112 (2014).
- [24] Aprem P. Joy and Achim Rosch, “Dynamics of visons and thermal Hall effect in perturbed Kitaev models,” *arXiv e-prints*, arXiv:2109.00250 (2021), arXiv:2109.00250 [cond-mat.str-el].
- [25] Yao-Dong Li, Xu Yang, Yi Zhou, and Gang Chen, “Non-kitaev spin liquids in kitaev materials,” *Phys. Rev. B* **99**, 205119 (2019).
- [26] Andrew M. Essin and Michael Hermele, “Classifying fractionalization: Symmetry classification of gapped F_2 spin liquids in two dimensions,” *Phys. Rev. B* **87**, 104406 (2013).
- [27] Michael Levin and Ady Stern, “Classification and analysis of two-dimensional abelian fractional topological insulators,” *Phys. Rev. B* **86**, 115131 (2012).
- [28] Maissam Barkeshli, Parsa Bonderson, Meng Cheng, and Zhenghan Wang, “Symmetry fractionalization, defects, and gauging of topological phases,” *Phys. Rev. B* **100**, 115147 (2019).
- [29] Yang Qi, Meng Cheng, and Chen Fang, “Symmetry fractionalization of visons in \mathbb{Z}_2 spin liquids,” *arXiv e-prints*, arXiv:1509.02927 (2015), arXiv:1509.02927 [cond-mat.str-el].
- [30] Peng Rao and Inti Sodemann, “Theory of weak symmetry breaking of translations in $z=2$ topologically ordered states and its relation to topological superconductivity from an exact lattice $z=2$ charge-flux attachment,” *Physical Review Research* **3**, 023120 (2021).
- [31] Xiao-Gang Wen, “Quantum order from string-net condensations and the origin of light and massless fermions,” *Phys. Rev. D* **68**, 065003 (2003).
- [32] Pok Man Tam, Jörn W. F. Venderbos, and Charles L. Kane, “Toric-code insulator enriched by translation symmetry,” *Phys. Rev. B* **105**, 045106 (2022).
- [33] Subir Sachdev and Matthias Vojta, “Translational symmetry breaking in two-dimensional antiferromagnets and superconductors,” *arXiv e-prints*, cond-mat/9910231 (1999), arXiv:cond-mat/9910231 [cond-mat.str-el].
- [34] T. Senthil and Matthew P. A. Fisher, “ \mathbb{Z}_2 gauge theory of electron fractionalization in strongly correlated systems,” *Phys. Rev. B* **62**, 7850–7881 (2000).
- [35] A Yu Kitaev, “Unpaired majorana fermions in quantum wires,” *Physics-Uspekhi* **44**, 131–136 (2001).
- [36] Michael Levin and Zheng-Cheng Gu, “Braiding statistics approach to symmetry-protected topological phases,” *Phys. Rev. B* **86**, 115109 (2012).
- [37] Chong Wang, L. Gioia, and A. A. Burkov, “Fractional quantum hall effect in weyl semimetals,” *Phys. Rev. Lett.* **124**, 096603 (2020).
- [38] A.Yu. Kitaev, “Fault-tolerant quantum computation by anyons,” *Annals of Physics* **303**, 2–30 (2003).
- [39] Di Xiao, Ming-Che Chang, and Qian Niu, “Berry phase effects on electronic properties,” *Rev. Mod. Phys.* **82**, 1959–2007 (2010).
- [40] Ryuichi Shindou, Ryo Matsumoto, Shuichi Murakami, and Jun-ichiro Ohe, “Topological chiral magnonic edge mode in a magnonic crystal,” *Phys. Rev. B* **87**, 174427 (2013).
- [41] Paul McClarty, “Topological Magnons: A Review,” *arXiv e-prints*, arXiv:2106.01430 (2021), arXiv:2106.01430 [cond-mat.str-el].
- [42] Chuan Chen, Peng Rao, and Inti Sodemann, “Berry Phases of Vison Transport in \mathbb{Z}_2 Topological Ordered States from Exact Fermion-Flux Lattice Dualities,” *arXiv e-prints*, arXiv:2202.01238 (2022), arXiv:2202.01238 [cond-mat.str-el].
- [43] R. Moessner and S. L. Sondhi, “Ising models of quantum frustration,” *Phys. Rev. B* **63**, 224401 (2001).
- [44] R. Moessner, S. L. Sondhi, and P. Chandra, “Two-dimensional periodic frustrated ising models in a transverse field,” *Phys. Rev. Lett.* **84**, 4457–4460 (2000).
- [45] E. Lefrancois, G. Grissonnanche, J. Baglo, P. Lampen-Kelley, J.-Q. Yan, C. Balz, D. Mandrus, S. E. Nagler, S. Kim, Young-June Kim, N. Doiron-Leyraud, and Louis Taillefer, “Evidence of a phonon hall effect in the kitaev spin liquid candidate α - rucl_3 ,” *Phys. Rev. X* **12**, 021025 (2022).
- [46] Mengxing Ye, Gábor B. Halász, Lucile Savary, and Leon Balents, “Quantization of the thermal hall conductivity at small hall angles,” *Phys. Rev. Lett.* **121**, 147201 (2018).
- [47] Yuval Vinkler-Aviv and Achim Rosch, “Approximately quantized thermal hall effect of chiral liquids coupled to phonons,” *Phys. Rev. X* **8**, 031032 (2018).
- [48] Jing-Yuan Chen, Steven A. Kivelson, and Xiao-Qi Sun, “Enhanced thermal hall effect in nearly ferroelectric insulators,” *Phys. Rev. Lett.* **124**, 167601 (2020).
- [49] Haoyu Guo and Subir Sachdev, “Extrinsic phonon ther-

- mal hall transport from hall viscosity,” *Phys. Rev. B* **103**, 205115 (2021).
- [50] Kai Klocke, Joel E. Moore, Jason Alicea, and Gábor B. Halász, “Thermal probes of phonon-coupled kitaev spin liquids: From accurate extraction of quantized edge transport to anyon interferometry,” *Phys. Rev. X* **12**, 011034 (2022).
- [51] Ryo Matsumoto and Shuichi Murakami, “Rotational motion of magnons and the thermal hall effect,” *Phys. Rev. B* **84**, 184406 (2011).
- [52] A. N. Ponomaryov, L. Zviagina, J. Wosnitza, P. Lampen-Kelley, A. Banerjee, J.-Q. Yan, C. A. Bridges, D. G. Mandrus, S. E. Nagler, and S. A. Zvyagin, “Nature of magnetic excitations in the high-field phase of α - ruiCl_3 ,” *Phys. Rev. Lett.* **125**, 037202 (2020).
- [53] Andrew M. Essin and Michael Hermele, “Spectroscopic signatures of crystal momentum fractionalization,” *Phys. Rev. B* **90**, 121102 (2014).
- [54] Andrés M. Somoza, Pablo Serna, and Adam Nahum, “Self-Dual Criticality in Three-Dimensional \mathbb{Z}_2 Gauge Theory with Matter,” *Physical Review X* **11**, 041008 (2021), arXiv:2012.15845 [cond-mat.stat-mech].